

REPORT DOCUMENTATION PAGE			Form Approved OMB No. 0704-0188	
<small>Public reporting burden for this collection of information is estimated to average 1 hour per response, including the time for reviewing instructions, searching existing data sources, gathering and maintaining the data needed, and completing and reviewing the collection of information. Send comments regarding this burden estimate or any other aspect of this collection of information, including suggestions for reducing this burden, to Washington Headquarters Services, Directorate for Information Operations and Reports, 1215 Jefferson Davis Highway, Suite 1204, Arlington, VA 22202-4302, and to the Office of Management and Budget, Paperwork Reduction Project (0704-0188), Washington, DC 20503.</small>				
1. AGENCY USE ONLY (Leave blank)		2. REPORT DATE		3. REPORT TYPE AND DATES COVERED FINAL REPORT - 1 Dec 92 - 30 Nov 95
4. TITLE AND SUBTITLE  Nucleation and Growth of Semiconductor-Metallic Superlattices			5. FUNDING NUMBERS  61102F 2305/ES	
6. AUTHOR(S)  P.I. Cohen				
7. PERFORMING ORGANIZATION NAME(S) AND ADDRESS(ES)  Department of Electrical Engineering University of Minnesota Minneapolis, MN 55455			8. PERFORMING ORGANIZATION REPORT NUMBER	
9. SPONSORING / MONITORING AGENCY NAME(S) AND ADDRESS(ES)  AFOSR/NE 110 Duncan Avenue Suite B115 Bolling AFB, DC 20332			10. SPONSORING / MONITORING AGENCY REPORT NUMBER  F49620-93-1-0080	
11. SUPPLEMENTARY NOTES				
19960726 023				
12a. DISTRIBUTION / AVAILABILITY STATEMENT  APPROVED FOR PUBLIC RELEASE: DISTRIBUTION UNLIMITED				
13. ABSTRACT (Maximum 200 words) An investigation of the nucleation and growth as well as magnetic properties of epitaxial FeAl on AlAs/GaAs(100) is reported. These are the first real space studies of the nucleation, growth and properties of so-called thermodynamically stable films. In-situ RHEED and the first UHV STM measurements were used to characterize the surface. Ex-situ MOKE measurements were used to characterize the magnetic properties. FeAl was found to have an unusual incubation effect over the first 3 bilayers of growth on AlAs. STM images taken at 1 and 3 bilayers examined this effect. After depositing 9 nm and annealing, the films exhibited a 2x2 and/or a 5x5 surface reconstruction. This reconstruction depended upon the anneal temperature and film composition. STM images showed atomic step terraces with step heights roughly corresponding to the height of an FeAl bilayer. Differences were also seen in the surface morphology of the 2-fold and 5-fold surfaces. It was determined that the growth mode was primarily dependent upon growth composition, but had some dependence on the annealed FeAl starting surface. The growth mode changed from monolayer to bilayer closely corresponding to the composition at which FeAl changes from ferromagnetic to non magnetic.				
14. SUBJECT TERMS  FeAl, Contacts, Superlattices			15. NUMBER OF PAGES	
			16. PRICE CODE	
17. SECURITY CLASSIFICATION OF REPORT Unclassified	18. SECURITY CLASSIFICATION OF THIS PAGE Unclassified	19. SECURITY CLASSIFICATION OF ABSTRACT Unclassified	20. LIMITATION OF ABSTRACT	

# Contents

<b>1</b>	<b>Abstract</b>	<b>2</b>
<b>2</b>	<b>Introduction</b>	<b>3</b>
<b>3</b>	<b>Experimental</b>	<b>4</b>
<b>4</b>	<b>Results and Discussion</b>	<b>5</b>
4.1	Nucleation . . . . .	5
4.2	Annealing . . . . .	6
4.3	Growth . . . . .	7
4.4	Magnetic Properties . . . . .	8
<b>5</b>	<b>Conclusion</b>	<b>8</b>
<b>6</b>	<b>References</b>	<b>9</b>

# 1 Abstract

An investigation of the nucleation and growth as well as magnetic properties of epitaxial  $\text{Fe}_x\text{Al}_{1-x}$  on AlAs/GaAs(100) is reported. In-situ RHEED and UHV STM were used to characterize the surface and ex-situ MOKE measurements were used to characterize the magnetic properties. We found that epitaxial films can be grown over a broad composition range  $0.5 < x < 0.8$  provided the appropriate nucleation procedure is used, most important of which is the deposition of more than  $90\text{\AA}$  of  $\text{Fe}_x\text{Al}_{1-x}$  before annealing.  $\text{Fe}_x\text{Al}_{1-x}$  undergoes an unusual incubation effect over the first 3 bilayers of growth on AlAs. STM images taken at 1 and 3 bilayers shed some light on why this incubation effect exists. After depositing  $90\text{\AA}$  and annealing, the films exhibited a  $2 \times 2$  and/or a  $5 \times 5$  surface reconstruction. This reconstruction depended upon the anneal temperature and film composition. STM images of a typical annealed film showed atomic step terraces with step heights roughly corresponding to the height of an  $\text{Fe}_x\text{Al}_{1-x}$  bilayer. Differences were also seen in the surface morphology of the 2-fold and 5-fold surfaces. Growth of  $\text{Fe}_x\text{Al}_{1-x}$  on an annealed  $\text{Fe}_x\text{Al}_{1-x}$  surface produced RHEED oscillations which were found to occur in 2 distinct modes, monolayer and bilayer. It was determined that this growth mode was primarily dependent upon growth composition, but had some dependence on the annealed  $\text{Fe}_x\text{Al}_{1-x}$  starting surface. The composition at which the growth mode changed from monolayer to bilayer closely corresponded to the composition at which  $\text{Fe}_x\text{Al}_{1-x}$  changes from ferromagnetic to nonmagnetic. Magnetic measurements of several samples confirmed samples above  $x = 0.7$  to be ferromagnetic with magnetization in-plane. A compositional dependence on coercivity and saturation magnetization was also found.

## 2 Introduction

The stable epitaxial growth of metals on III-V's is important to metal/semiconductor devices that need to operate at high temperature and to buried metal layer devices where interdiffusion at interfaces cannot be permitted. However, most metals that can be grown epitaxially on III-V's are not thermodynamically stable so that even modest heating causes reaction and interdiffusion at the interface. Sands et al. [1] have reviewed these issues and discussed other criteria necessary for stable epitaxial growth of metals on III-Vs. The main conclusion is that binary intermetallics that are lattice matched to III-V's and which can coexist with the III-V according to bulk phase diagram are candidate materials. Experiment has confirmed many of these ideas [1], but the interplay of kinetics and thermodynamics as well as the details of the growth mechanisms has not been worked out. The main purpose of this paper is to combine scanning tunneling microscopy (STM) with reflection high energy electron diffraction (RHEED) to study these competing issues.

Two major groups of intermetallics have been found to form stable epitaxial films. The first group has a cubic CsCl (B2) crystal structure and are known collectively as transition metal - three (TM-III) intermetallics. Some notable examples include NiAl, CoAl, FeAl, NiGa and CoGa. Their lattice parameters are usually 1-3% larger than one half the lattice parameter of GaAs and their CsCl phases usually exists over a wide composition range. For  $\text{Fe}_x\text{Al}_{1-x}$  the lattice mismatch is 2.9% and the range over which the phase exist is  $0.5 < x < 0.63$ . The second major group has a NaCl (B1) structure and are known collectively as rare earth - five (RE-V) intermetallics. Some notable examples include ErAs, LuAs and (Sc,Er)As. Their lattice mismatch is generally smaller, less than 2%. In this paper we examine the  $\text{Fe}_x\text{Al}_{1-x}$  system because, in addition to the CsCl phase, it has a stable  $\text{BiF}_3$  ( $\text{DO}_3$ ) phase that is also reasonably well lattice matched to GaAs. This  $\text{BiF}_3$  phase exists over the composition range,  $0.63 < x < 0.78$  [2] and has a lattice mismatch of 2.4% [3]. It has been shown to form stable epitaxial films on AlAs up to 550°C [4, 5] and has even been successfully grown directly on GaAs [6, 7].  $\text{Fe}_x\text{Al}_{1-x}$  is particularly interesting since it becomes ferromagnetic at compositions above  $x=0.7$ . This makes it possible for  $\text{Fe}_x\text{Al}_{1-x}$  to be used for magnetic metal/semiconductor devices. Further, its magnetic properties can be varied in a given structure simply by varying its composition.

In this paper we investigate nucleation, annealing, growth and magnetic properties of  $\text{Fe}_x\text{Al}_{1-x}$  films spanning both the CsCl and  $\text{BiF}_3$  composition range,  $0.5 < x < 0.78$ . Previous work by Kuznia and Wowchak used RHEED and Auger electron spectroscopy to study the nucleation and growth of  $\text{Fe}_x\text{Al}_{1-x}$  on pseudomorphic AlAs on InP(100) [4] and on AlAs/GaAs(100) [5]. They reported several main results.

First, the initial nucleation exhibits an incubation period lasting 2 to 3 bilayers in which the intensity of the diffraction pattern decreases to near zero and then recovers. Second, growth of  $\text{Fe}_x\text{Al}_{1-x}$  on an annealed  $\text{Fe}_x\text{Al}_{1-x}$  surface results in RHEED oscillations corresponding to the growth of a monolayer or a bilayer of  $\text{Fe}_x\text{Al}_{1-x}$ . As seen in Fig.1, a monolayer is defined as a one atom thick layer and a bilayer is defined as a two atom thick layer. In that work, however, it was difficult to extract quantitative information on surface morphology from the RHEED measurements, especially in the nucleation stage where the diffraction was weak and diffuse. In this work, we have applied ultrahigh vacuum STM to obtain a real space view of the surface. We are able to use STM to examine a surface in which the RHEED pattern was diffuse. We use STM to extract step height and mean terrace lengths. In addition, we studied annealing and growth in more detail. Finally, we studied the magnetic properties of the films.

### 3 Experimental

A PHI-400 solid source MBE system was used for growth. Standard Knudsen cells were used for all sources except Fe. An e-beam source specially designed to fit in a source port was used for Fe. This e-beam source is similar to that described by Jonker et-al [8]. The system was also equipped with a quartz crystal deposition monitor which could be positioned directly in front of the substrate. This was found to produce a much more accurate flux calibration for the e-beam source than an ion gauge or a mass spectrometer. In-situ growth monitoring was performed with a 10 KeV RHEED system. The STM was housed in a separate chamber attached to the growth chamber. Samples could be transferred to this chamber without exposure to pressures above  $1 \times 10^{-8}$  Torr. MOKE measurements, specifically longitudinal and polar Kerr hysteresis loops, were performed in air.

Epi-ready GaAs(100)  $n^+$  Si doped samples were cleaned by desorbing the oxide at  $620^\circ\text{C}$  in an  $\text{As}_4$  background of  $1 \times 10^{-6}$  Torr. A 3000 Å GaAs buffer, doped with Si to about  $1 \times 10^{18} \text{ cm}^{-3}$ , was then grown. The buffer and substrate were doped to ensure that the sample would be conducting for STM measurements. After the GaAs buffer, 10 monolayers of AlAs was deposited at  $540^\circ\text{C}$ . With AlAs as an effective substrate, the thermodynamic stability argument regarding a three element system is expected to apply. The sample was cooled to  $200^\circ\text{C}$  and removed from the deposition chamber. The Arsenic source was cooled and the remaining Arsenic background was gettered with Ga and Al until the base pressure was below  $3 \times 10^{-9}$  Torr. The Fe and Al sources were then set to give the desired Fe-Al ratio using the quartz crystal deposition rate monitor. The sample was then returned to the deposition chamber and heated to  $700^\circ\text{C}$  until an AlAs ( $3 \times 2$ ) pattern appeared.

This procedure was shown to drive off Ga surface contaminants and to reduce the Arsenic coverage on the surface [9]. Finally, the sample temperature was brought back down to 200°C and  $\text{Fe}_x\text{Al}_{1-x}$  was grown by co-deposition of Fe and Al.

To produce an epitaxial film, we deposited a minimum of 90 Å of  $\text{Fe}_x\text{Al}_{1-x}$  on the AlAs surface before annealing to between 550 and 700°C. After annealing, additional  $\text{Fe}_x\text{Al}_{1-x}$  was grown at 200°C by again co-depositing Fe and Al. After growth of about 100 Å, the film would again be annealed to between 550 and 700°C. This process of growth and annealing could be repeated indefinitely without degradation of the RHEED pattern.

## 4 Results and Discussion

### 4.1 Nucleation

The intensity of the specular diffracted beam is shown versus time during the initial growth of FeAl on an AlAs buffer, Fig. 2. Here,  $\text{Fe}_x\text{Al}_{1-x}$  is co-deposited at a rate of 0.25 monolayers per second which corresponds to a period of 4.06 seconds per monolayer. The nucleation of the film is characterized by a near complete drop in the diffracted intensity followed shortly thereafter by a recovery and, in some cases, weak intensity oscillations. The starting RHEED pattern at  $t_1$  is an AlAs ( $3 \times 2$ ). At  $t_2$ , after about 1 - 2 monolayers of deposition, the pattern is gone and the RHEED exhibits only a diffuse background. With continued deposition a weak  $1 \times 1$   $\text{Fe}_x\text{Al}_{1-x}$  pattern begins to develop. At  $t_3$ , after 6 monolayers of deposition, the  $1 \times 1$  pattern is now between 30 and 50% of the original intensity and remains near this intensity with continued deposition. The time period over which the diffraction pattern remains near zero is termed the incubation period and the time between when the pattern begins to recover and is fully recovered is termed the recovery period.

Fig. 3a and b shows STM images taken after roughly 2 monolayers of growth. This corresponds to the point in the nucleation where the RHEED pattern intensity is a minimum. The first image, Fig. 3a, shows a long range scan. Large terraces, some greater than 120nm in size, can be seen in this image. A close range scan, Fig. 3b, shows that the entire surface is covered with small features, 40 Å in size and approximately 2 Å high. These small features do not appear to be clearly resolved. Based on prior experience, this is likely due to a dull STM tip. Because of this, the real height values may be somewhat larger than the measure values. We interpret the large terraces observed in Fig. 3a to be due to the underlying AlAs surface and the small features due to  $\text{Fe}_x\text{Al}_{1-x}$  clusters. We base this statement on the fact that

similar shaped terraces have been observed on a clean AlAs ( $3 \times 2$ ) surface. From this STM image and noting that there is no RHEED pattern, we postulate that the small clusters are either highly disordered or randomly oriented on the AlAs surface.

## 4.2 Annealing

At least 90 Å, roughly 30 bilayers, of  $\text{Fe}_x\text{Al}_{1-x}$  was deposited on the AlAs surface at 200°C before annealing. Annealing films less than 90 Å thick commonly resulted in the formation of a surface pattern that lacked a bright central spot, characteristic of a sharp diffraction. We interpreted this to mean that the surface was ordered on a short range but was not well ordered on a long range. It was not possible to obtain RHEED oscillations on such a surface nor was it possible to recover a sharp diffraction pattern by depositing additional  $\text{Fe}_x\text{Al}_{1-x}$  and annealing. The 90 Å thickness was only a thickness that we found gave us good results for all film compositions. At lower Fe compositions, closer to  $x=0.5$ , we were able to anneal films as thin as 20 Å, roughly 6 bilayers, with satisfactory results. In no cases were we able to anneal films less than 20 Å thick and get a sharp diffraction pattern. We are uncertain why this effect is observed, but can postulate that it is due to either a reaction at the interface, a dewetting effect or a lattice strain relaxation effect.

After growing approximately 100 Å at low temperatures, the films were annealed because, as grown, the RHEED pattern exhibited a broad and diffuse  $1 \times 1$  diffraction pattern. This type of diffraction pattern is indicative of a rough surface with many defects. After annealing, the films exhibited either a sharp  $2 \times 2$  and/or a sharp  $5 \times 5$  diffraction pattern. A sharp  $2 \times 2$  pattern would appear after annealing to 550°C for 5 min. The appearance of this pattern was not dependent on composition. However, annealing films to 650-700°C resulted in the composition dependent formation of a  $2 \times 2$  and/or a  $5 \times 5$  diffraction pattern. At  $x = 0.5$ , the film would exhibit a pure  $2 \times 2$  pattern. Between  $0.55 < x < 0.7$  the film would exhibit a combined  $2 \times 2$  and  $5 \times 5$  pattern with the 5-fold pattern becoming more and more dominant at higher Fe concentrations. This combined RHEED pattern was most likely caused by the surface having regions of 5-fold ordering and other regions of 2-fold ordering. At or above  $x = 0.75$ , the film would exhibit a pure  $5 \times 5$  pattern.

We looked at the surface of two annealed films with UHV STM, one exhibiting a  $2 \times 2$  diffraction pattern and one exhibiting a  $5 \times 5$  pattern. Fig 4a and 4b show the images corresponding to the  $2 \times 2$  surface. This film had the composition  $\text{Fe}_{0.72}\text{Al}_{0.28}$  and was annealed to approximately 550°C. Islands and terraces are clearly visible. The average island size is about 150 Å and average step heights is about 3 Å which roughly corresponds to one half the  $\text{Fe}_3\text{Al}$  lattice constant, 2.89 Å. Fig. 4c and 4d) show STM images corresponding to a  $5 \times 5$  surface. This film

had the composition  $\text{Fe}_{0.76}\text{Al}_{0.24}$  and was annealed to approximately 650-700°C. Here, few islands are visible, but terraces can be seen. The average terrace length is about 400 Å and the measured step height is approximately 3 Å. Comparing the two images, it is clear that the  $5 \times 5$  has a much smaller step density than the  $2 \times 2$  surface as is expected by a higher temperature anneal. However, the  $5 \times 5$  surface also exhibits faceting along the  $(0\bar{1}1)$  and the  $(011)$  directions causing the appearance of sharp 90° kinks in the step edges of the terraces.

### 4.3 Growth

After annealing,  $\text{Fe}_x\text{Al}_{1-x}$  was deposited on the annealed  $\text{Fe}_x\text{Al}_{1-x}$  surface. Depending on the growth composition and the annealed surface, two different growth modes were observed, monolayer and bilayer, as determined by RHEED oscillations. Compositions between  $0.7 < x < 0.8$  always resulted in monolayer growth while compositions between  $0.5 < x < 0.7$  resulted in either bilayer or a combined monolayer and bilayer growth. In this composition range, the annealed surface upon which we were growing had a large effect on growth mode. On a  $2 \times 2$  surface, growth would be bilayer, however when attempting to grow on a surface exhibiting a  $5 \times 5$  diffraction pattern, at least the first few oscillations would be monolayer growth. The duration of the monolayer growth was dependent on the growth composition. For example, if we grew at a composition of  $x = 0.6$  on a  $5 \times 5$  surface, the first 10-12 oscillations would be monolayer oscillations. At a composition of  $x = 0.5$ , only the first 1 or 2 oscillations would be monolayer oscillations. After the monolayer oscillations, the growth would then make a transition back to bilayer growth. Fig. 5 shows RHEED oscillations at various compositions on a  $5 \times 5$  surface. Note that even at  $x = 0.51$ , the first oscillation is a monolayer oscillation and that as we increase the composition, the monolayer oscillations persist longer. The fact that the magnitude of the oscillations generally started out small and got larger was due to the diffraction beam moving into the detection area of the photomultiplier. This beam wandering effect may have been due to the changing magnetic properties of the film. The decrease in intensity is due to surface roughening and is an artifact of RHEED oscillations.

From the results of growth on a  $5 \times 5$  surface, we conclude that this surface must have excess Fe on it and this excess Fe gets incorporated into growth, changing the stoichiometry of the growth front enough to cause monolayer oscillations. We postulate that the Fe incorporates to a saturation level, probably around  $x = 0.75$ , and any Fe not incorporated into the current layer would continue to ride the surface and be incorporated into the following layers. This would cause monolayer oscillations to continue until the excess Fe was used up at which point the growth



mode would transition back to bilayer. It follows that the amount of growth needed before the oscillations would change to bilayer would be dependent on the growth composition. If growing low Fe concentration, the excess Fe would be incorporated quickly and the oscillation would transition to bilayer quickly. If growing higher Fe concentrations, the excess Fe would be incorporated more slowly and the transition to bilayer oscillation would take longer.

## 4.4 Magnetic Properties

The magnetic properties of several films were examined to see if they possessed magnetic properties that may be of interest for magnetic devices as well as to check if the films possessed the expected magnetic properties. Several samples spanning the composition range from ferromagnetic to non-magnetic were measured. Fig. 6 shows the longitudinal Kerr measurements of these samples. The longitudinal Kerr rotation is a measure of the in-plane magnetization of the film. These measurements show that the  $x = 0.6$  sample was non-magnetic as expected. Both of the films that were ferromagnetic showed 100% in-plane remanence. The  $x = 0.8$  sample showed a coercivity of  $H_c = 75$  Oe and the  $x = 0.7$  sample showed a coercivity of about  $H_c = 12$  Oe. From polar Kerr measurements, we found that the saturation field and maximum Kerr rotation were dependent on composition as well. For the  $x = 0.8$  sample,  $H_s = 16$  KOe and  $\theta_k = 0.228^\circ$  whereas for  $x = 0.7$  sample,  $H_s = 4.5$  KOe and  $\theta_k = 0.10^\circ$ .

## 5 Conclusion

We report on findings related to the nucleation, annealing, growth and magnetic properties of epitaxial  $\text{Fe}_x\text{Al}_{1-x}$  on AlAs/GaAs. First,  $\text{Fe}_x\text{Al}_{1-x}$  nucleates on an AlAs ( $3 \times 2$ ) surface in small clusters that are likely amorphous. Second, it is necessary to grow a minimum thickness of  $\text{Fe}_x\text{Al}_{1-x}$  on AlAs at low temperatures before annealing in order to obtain a surface with good long range ordering. It is unknown, at present, why thinner films can not be annealed. Third, the growth mode of  $\text{Fe}_x\text{Al}_{1-x}$  on an annealed  $\text{Fe}_x\text{Al}_{1-x}$  surface is primarily determined by growth composition. Monolayer growth occurs above  $x = 0.7$  and bilayer growth occurs below that value. However, the exact growth behavior also depends upon the surface being grown on, where a  $5 \times 5$  surface can force monolayer growth for at least several layers. This is likely due to the 5-fold surface being Fe rich. Finally, samples with  $x > 0.7$  were shown to be ferromagnetic with 100% in-plane magnetization.  $H_c$ ,  $M_s$  and  $\theta_k$  were found to be dependent on the Fe-Al ratio where all three increase with

increasing Fe concentration.

## 6 References

- [1] T. Sands, C.J. Palmstrom, J.P. Harbison, V.G. Keramidas, N. Tabatabaie, T.L. Cheeks, R. Ramesh and Y. Silberberg, *Mat. Sci. Rep.* 5, 99 (1990)
- [2] *Binary Alloy Phase Diagrams*, edited by T.B. Massalski (ASM, Metals Park, OH, 1986) p. 148
- [3] P. Villars and L.D. Calvert, "Pearson's Handbook of Crystallographic Data for Intermetallic Phases" (American Society for Metals, Metal Parkm Ohio, 1985), Vol 2.
- [4] A.M. Wowchak, J.N. Kuznia and P.I. Cohen, *J. Vacuum Sci. Technol. B* 7 (1989) 733
- [5] J.N. Kuznia, A.M. Wowchak and P.I. Cohen, *J. of Elect. Mat.* 19 (6), 561 (1990)
- [6] S.H. Liou, S.S. Malhotra, J.X. Shen, M. Hong, J. Kwo, H.S. Chen and J.P. Mannaerts, *J. Appl. Phys.* 73 (10), 6766 (1993)
- [7] M. Hong, H.S. CHen, J. Lwo, A.R. Kortan, J.P. Mannaerts, B.E. Weir and L.C. Feldman, *J. Crystal Growth* 111, 984 (1991)
- [8] B.T. Jonker, *J Vacuum Science* 8 (5), 3883-6 (1990)
- [9] A.M. Dabiran, P.I. Cohen, *J. Crystal Growth* 150, 23-27 (1995)

## Figure Captions

Fig. 1 Diagram showing an AlAs monolayer,  $d_1$  and an FeAl monolayer,  $d_2$  and an FeAl bilayer,  $d_3$ .

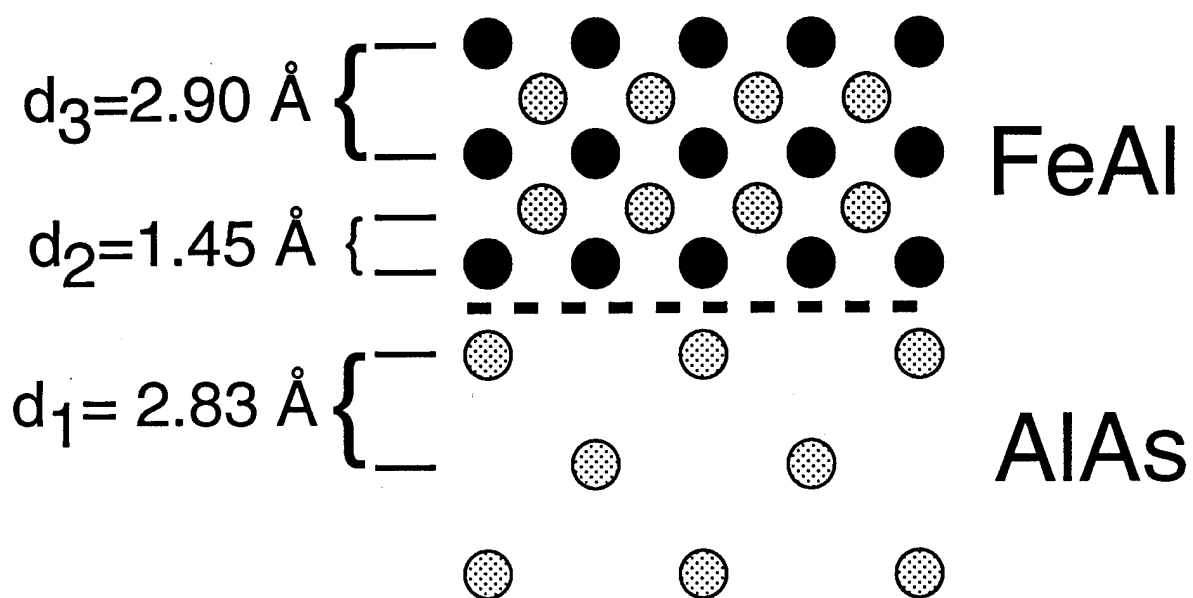
Fig. 2 RHEED intensity of the specular diffraction beam during initial nucleation of  $\text{Fe}_x\text{Al}_{1-x}$  on AlAs. The starting pattern at  $t_1$  is an AlAs ( $3 \times 2$ ) pattern. Growth is started at  $t_1$ . At time  $t_2$ , the RHEED pattern is no longer visible. At time  $t_3$ , the intensity recovers to 30% of the original intensity and exhibits a broad and diffused  $1 \times 1$  pattern.

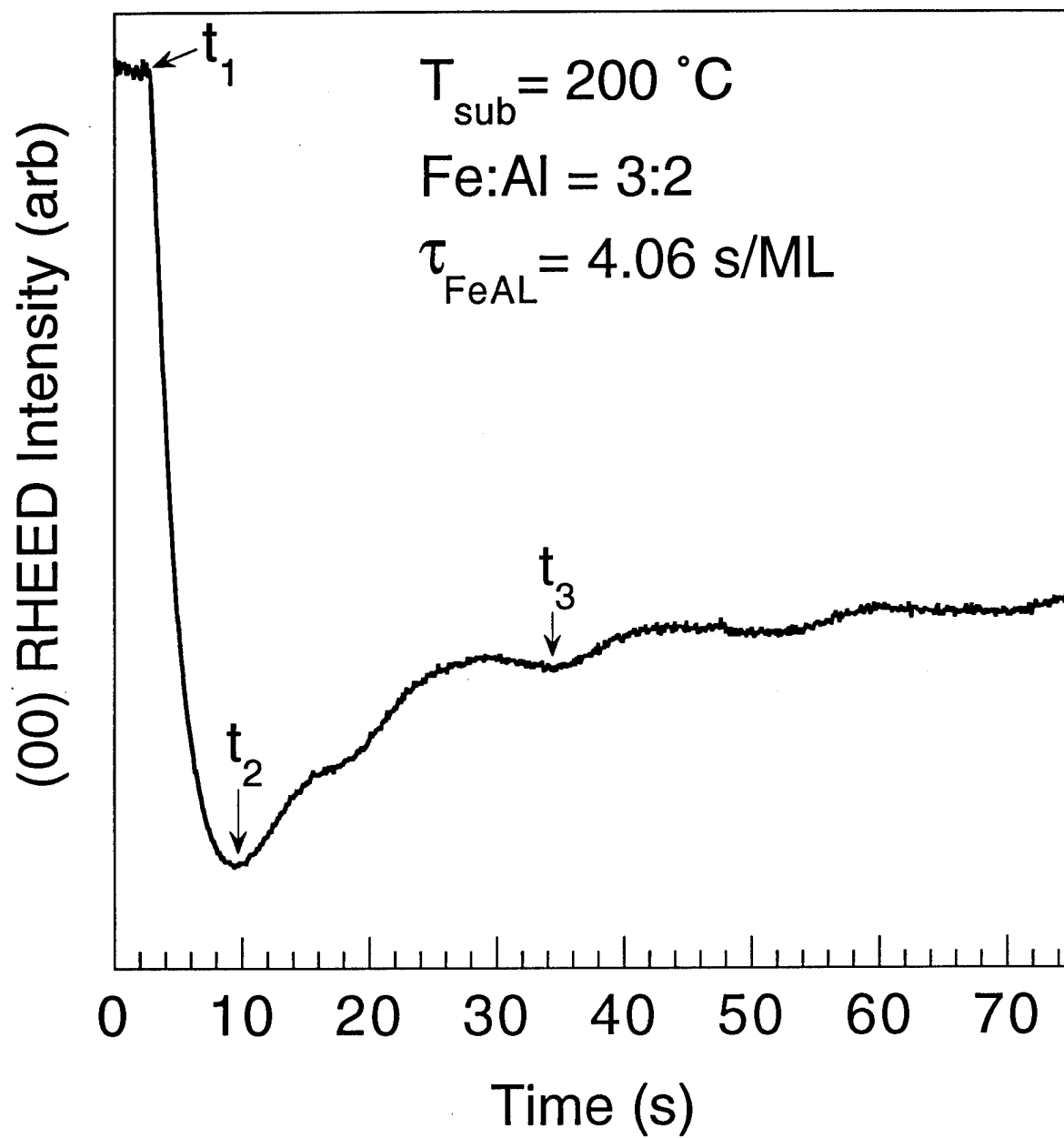
Fig. 3 STM images taken after 2 monolayers of growth. Terraces from the underlying AlAs surface can be seen in a) and small clusters of  $\text{Fe}_x\text{Al}_{1-x}$  can be seen in b).

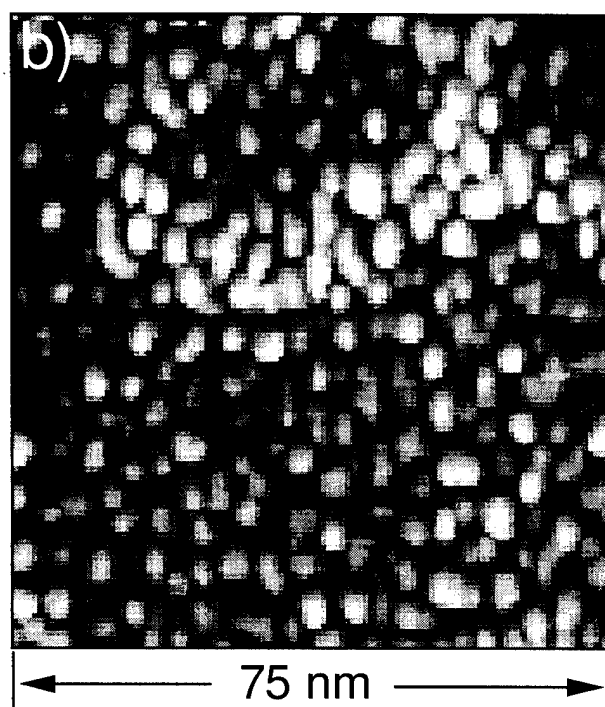
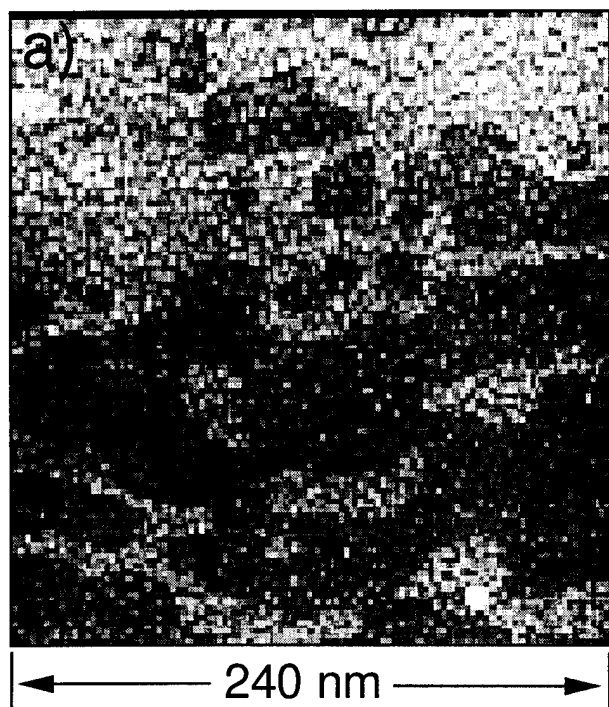
Fig. 4 Two STM images of an  $\text{Fe}_{0.72}\text{Al}_{0.28}$  surface annealed to approximately  $550^\circ\text{C}$ , a) and b), and two of an  $\text{Fe}_{0.74}\text{Al}_{0.24}$  surface annealed to approximately  $650\text{-}700^\circ\text{C}$ , c) and d). The sample from a) and b) exhibited a  $2 \times 2$  diffraction pattern while from c) and d) exhibited a  $5 \times 5$  diffraction pattern. Both surface exhibited bilayer high steps, but the step density in c) and d) is much smaller than in a) and b). Notice also the faceting in c) and d).

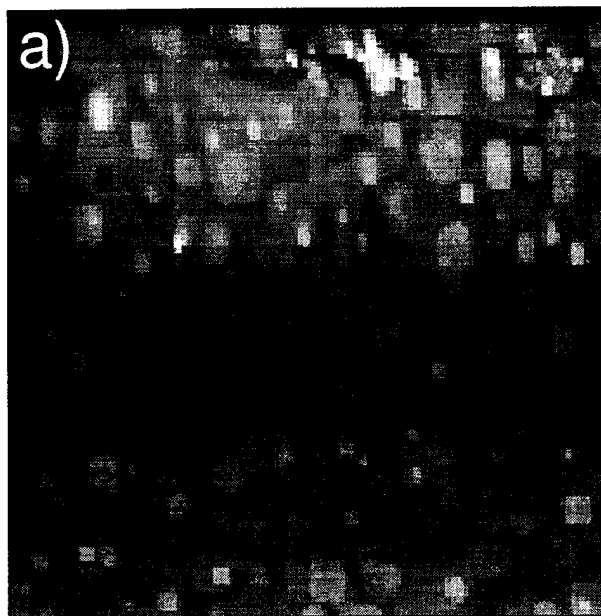
Fig. 5 RHEED oscillations due to growth on an annealed  $\text{Fe}_x\text{Al}_{1-x}$  surface which exhibits a  $5 \times 5$  diffraction pattern. It can be seen in that at a growth composition of  $x=0.51$ , the first oscillation is a monolayer oscillation and after are bilayer oscillations. At higher Fe concentrations, the monolayer oscillations last longer until above  $x=0.7$  where only monolayer oscillations are observed.

Fig. 6 Longitudinal Kerr loops of three samples of different compositions a)  $x=0.8$ , b)  $x=0.7$  and c)  $x=0.6$ . The  $x=0.6$  sample does not show Kerr rotation because it is non-magnetic. The other 2 samples are magnetic and show 100% in-plane remanence and a very quick magnetization reversal. The applied field at which the magnetization reverses is related to coercivity and it can be seen that the two samples have different coercivities.

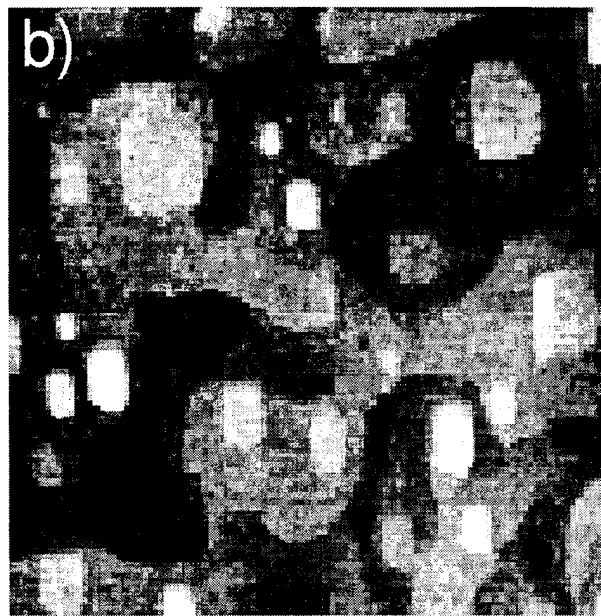




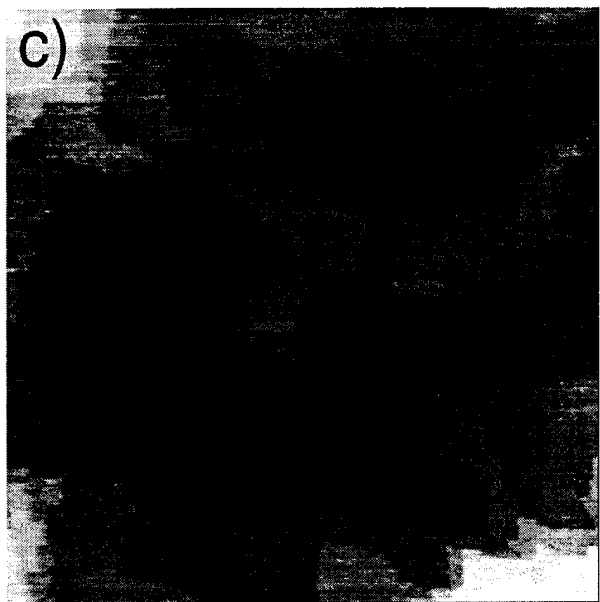




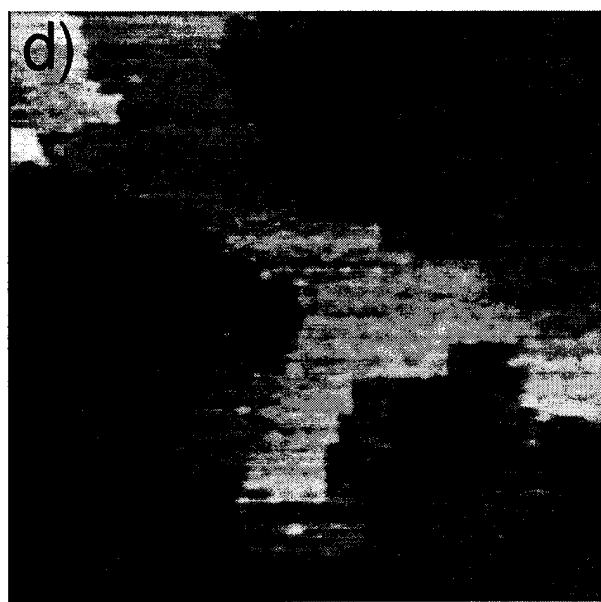
← 400 nm →



← 200 nm →



← 400 nm →



← 200 nm →

